

A Cannonball Model of Cosmic Rays

A. De Rújula^a

^aTheory Division, CERN; 1211 Geneva 23, Switzerland
Physics Department, Boston University, USA

I outline a *Cannon Ball* model of Cosmic Rays in which their distribution in the Galaxy, their total “luminosity”, the broken power-law spectra with their observed slopes, the position of the knee(s) and ankle(s), and the alleged variations of composition with energy are all explained in terms of simple and “standard” physics.

1. Credits

The *Cannonball* (CB) model is a unified model of high-energy astrophysics, in which the gamma background radiation, cluster “cooling flows”, gamma-ray bursts, X-ray flashes and cosmic-ray electrons and nuclei of all energies —share a common origin. The mechanism underlying all these phenomena is the emission of relativistic “cannonballs” by ordinary supernovae, analogous to the observed ejection of plasmoids by quasars and microquasars. It is not unusual in talks to start with the credits, as in a film. Many of the ideas I shall exploit have a long pedigree: Gamma-Ray Bursts (GRBs) are the main (injection) process for Cosmic Rays [1] (CRs); GRBs are the main CR (production and acceleration) mechanism [2], and are induced by narrow jets emitted by accreting compact stellar objects [3]; their γ -rays being low-energy photons boosted to higher energies by inverse Compton scattering [3] (ICS). The concrete realization of these ideas in the “Cannon-Ball” (CB) model is more recent and covers GRBs [4,5], X-Ray Flashes [6] (XRFs), their respective afterglows [7,8], the Gamma “Background” Radiation [9], the CR luminosity of our Galaxy [10], the “Cooling Flows” of galaxy clusters [11], and the properties of CRs [2,12,13].

2. Jets in Astrophysics

A look at the sky, or a more modest one at the web, results in the realization that jets are emitted by many astrophysical systems (stars,

quasars, microquasars...). One impressive case [14] is that of the quasar Pictor A, shown in Fig. 1. *Somehow*, the active galactic nucleus of this object is discontinuously spitting *something* that does not appear to expand sideways before it stops and blows up, having by then travelled for a distance of several times the visible radius of a galaxy. Many such systems have been observed. They are very relativistic: the Lorentz factors (LFs) $\gamma \equiv E/(mc^2)$ of their ejecta are typically of $\mathcal{O}(10)$. The mechanism responsible for these mighty ejections —suspected to be due to episodes of violent accretion into a very massive black hole— is not understood.

In our galaxy there are “micro-quasars”, in which the central black hole has only a few times the mass of the Sun. The first example [15] was the γ -ray source GRS 1915+105. Aperiodically, about once a month, it emits two opposite *cannonballs*, travelling at $v \sim 0.92c$. As the event takes place, the X-ray emission —attributed to an unstable accretion disk— temporarily decreases. How part of the accreting material ends up ejected along the system’s axis is not understood. The process reminds one of the blobs emitted upwards as the water closes into the “hole” made by a stone dropped onto its surface. For quasars and μ -quasars, it is only the relativistic, general-relativistic magneto-hydro-dynamic details that remain to be filled in! Atomic lines from many elements have been observed [16] in the CBs of μ -quasar SS 433. Thus, at least in this case, the ejecta are made of ordinary matter, and not of some fancier substance such as e^+e^- pairs.

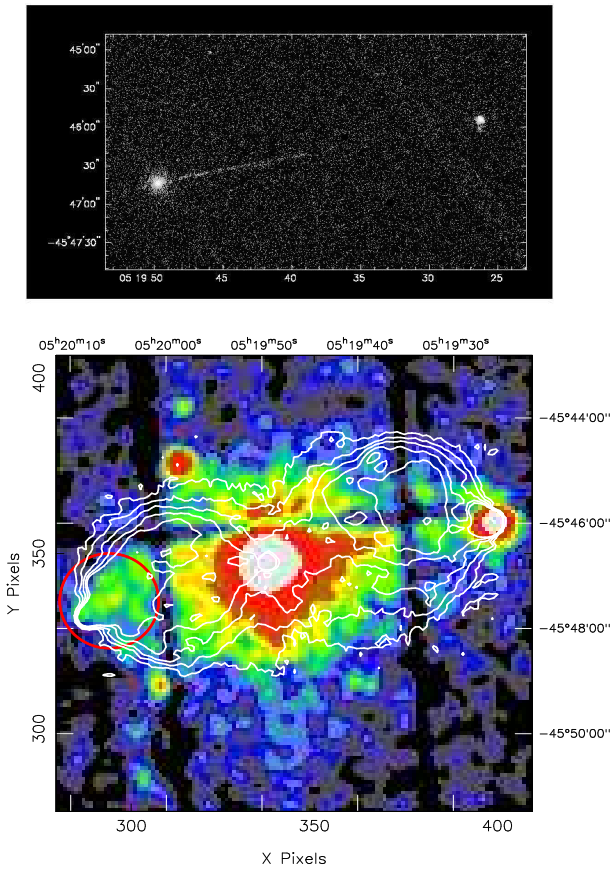


Figure 1. Above: X-ray image of the galaxy Pictor A: a non-expanding jet extends across 360000 light years towards a hot spot at least 800000 light years away from where the jet originates. Below: XMM/p-n image of Pictor A in the 0.2–12 keV energy interval, centred at the position of the leftmost spot in the upper panel, superimposed on the radio contours of a 1.4 GHz radio VLA map.

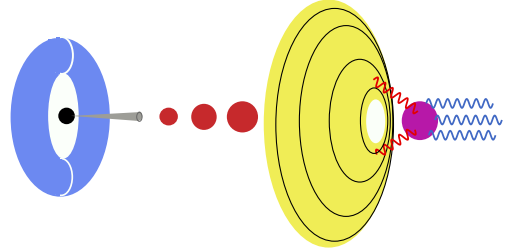


Figure 2. The CB model of long-duration GRBs [4]. A core-collapse SN results in a compact object and a fast-rotating torus of non-ejected fallen-back material. Matter (not shown) abruptly accreting into the central object produces a narrowly-collimated beam of CBs, of which only some of the “northern” ones are depicted. As these CBs move through the “ambient light” surrounding the star, they Compton up-scatter its photons to GRB energies [5].

3. The Cannonball Model

The “cannon” of the CB model is analogous to the ones responsible for the ejecta of quasars and microquasars. *Long-duration* GRBs, for instance, are produced in *ordinary core-collapse* supernovae (SNe) by jets of CBs, made of *ordinary-matter plasma*, and travelling with high Lorentz factors (LFs), $\gamma \sim \mathcal{O}(10^3)$. An accretion torus is hypothesized to be produced around the newly-born compact object, either by stellar material originally close to the surface of the imploding core and left behind by the explosion-generating outgoing shock, or by more distant stellar matter falling back after its passage [17,4]. A CB is emitted, as observed in microquasars [15], when part of the accretion disk falls abruptly onto the compact object, see Fig. 2.

Do supernovae emit cannonballs? Up to last year, there was only one case in which the data was good enough to tell: SN1987A, the core-collapse SN in the LMC, whose neutrino emission was detected. Speckle interferometry measurements made 30 and 38 days after the explosion [18] did show two relativistic CBs (one of them “superluminal”), emitted in opposite directions, as shown in Fig. 3.

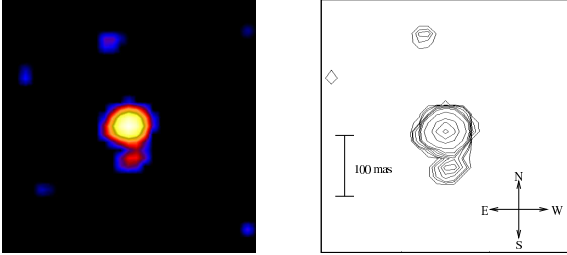


Figure 3. The two CBs emitted by SN1987A in opposite axial directions. The northern and southern bright spots are compatible with CBs emitted at the time of the SN explosion and travelling at a velocity equal, within errors, to c . One of the *apparent* velocities is superluminal. The corresponding GRBs were not pointing in our direction, which may have been a blessing.

4. GRB Afterglows and Cosmic Rays

A freshly jetted CB is assumed to be expanding at a speed comparable to that of sound in a relativistic plasma ($c/\sqrt{3}$). Its typical baryon number is that of half of Mercury, $N_{CB} \sim 10^{50}$, its start-up LF is $\gamma_0 \sim 10^3$ (both ascertained from the properties of afterglows (AGs), and of the GRB’s γ rays). In their voyage, CBs intercept the electrons and nuclei of the interstellar medium (ISM), previously ionized by the GRB’s γ rays. In seconds of (highly Doppler-foreshortened) observer’s time, such an expanding CB becomes “collisionless”, that is, its radius becomes bigger than a typical nucleus-nucleus interaction length. But it still interacts with the charged ISM particles it encounters, for it contains a magnetic field¹.

If the nuclei entering a CB are magnetically “scrambled” and are reemitted isotropically in the CB’s rest system, a radial loss of momentum results. The rate of such a loss corresponds to an

¹Numerical analysis of the merging of two plasmas at a high relative γ , based on following each particle’s individual trajectories as governed by the Lorentz force and Maxwell’s equations, demonstrate the generation of such turbulent magnetic fields, as well as the “Fermi” acceleration of particles, in the total *absence* of shocks [19], to a power law spectrum: $dN/dE \approx E^{-\beta_s}$, with $\beta_s \sim 2.2$.

inwards radial force on the CB. In our analysis of GRB AGs, we assumed that this force counteracts the expansion, and that when the radius stabilizes, the inwards pressure is in equilibrium with the pressure of the CB’s magnetic field. This results in values for the asymptotic CB radius ($R_{CB} \sim 10^{14}$ cm for typical parameters) and its time-dependent magnetic-field strength [8]:

$$B_{CB}[\gamma(t)] = 3 \text{ Gauss} \frac{\gamma(t)}{10^3} \left(\frac{n_p}{10^{-3} \text{ cm}^{-3}} \right)^{1/2}, \quad (1)$$

where n_p is the ISM number density, normalized to a value characteristic of the “superbubble” domains in which SNe and GRBs are born. Our assumptions are no doubt naïve, but they are to be judged in light of two facts: 1) The very simple ensuing analysis [7,8] of the elaborate time and frequency dependence of AGs, dominated by electron synchrotron radiation of in the field of Eq. (1); 2) The CBs emitted by certain objects appear not to expand significantly, as in the example in the upper part of Fig. 1.

As a CB pierces through the ISM, its LF, $\gamma(t)$, continuously diminishes, as its energy is dominantly transferred to scattered ISM nuclei, and subdominantly to scattered electrons and synchrotron photons. All these reemitted particles, in the rest system of the host galaxy, are forward-peaked in distributions of characteristic opening angle $1/\gamma(t)$. In the lower Fig. 1 the two jets of Pictor A are shown, with contour plots corresponding to radio-intensity levels [20]. We interpret this radio signal as the synchrotron radiation of the CB-generated *Cosmic-Ray electrons* in the ambient magnetic fields. The CBs of Pictor A must also be scattering the intercepted nuclei, and converting them into *Cosmic-Ray Nuclei*.

The range of a CB is governed by the rate at which it loses momentum by encountering ISM particles and catapulting them into CRs. The initial LF, $\gamma_0 \sim 10^3$, is typically halved in a fraction of a kpc, while a CB becomes non-relativistic only at distances of 10’s or even 100’s of kpc, well into a galaxy’s halo or beyond. The CRs of the CB model are deposited along the long *line* of flight of CBs, in contradistinction with those of the standard models, in which the CRs are generated by SN shocks, at the “*points*” where they occur in

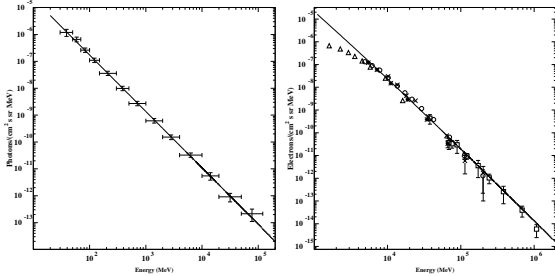


Figure 4. Left: Comparison between the spectrum of the GBR, measured by EGRET, and the prediction (the line) for ICS of starlight and the CMB by CR electrons. Right: The primary CR electron spectrum. The slope is the prediction, the magnitude is normalized to the data.

“active” regions of stellar birth and death. In the CB model no reacceleration far from the CR birth-sites need be invoked to accommodate the data. This is most relevant for electrons, which lose energy fast, and locally [9].

5. The “GBR” and the CR electrons

The existence of an isotropic, diffuse gamma background radiation (GBR, confusingly similar to GRB) was first suggested by data from the SAS 2 satellite [21]. The EGRET/CRGO instrument confirmed it: “*by removal of point sources and of the galactic-disk and galactic-centre emission, and after an extrapolation to zero local column density*”, a uniformly distributed GBR was found, of alleged extragalactic origin [22]. Above an energy of ~ 10 MeV, this radiation has a featureless spectrum, shown in Fig. 4, which is very well described by a simple power-law form, $dF/dE \propto E^{-\beta_{\text{GBR}}}$, with $\beta_{\text{GBR}} \approx 2.10 \pm 0.03$.

There is no consensus on what the origin of the GBR is. The proposed candidate sources range from the rather conventional (e.g. active galaxies [23]) to the decisively speculative (e.g. primordial black hole evaporation [24]). A “cosmological” origin is the most noble putative ancestry, but though the GBR index β_{GBR} is uncannily direction-independent, the EGRET GBR flux in directions above the galactic disk and cen-

tre shows significant anisotropies, correlated with our position relative to the centre of the Galaxy [25]. How does the GBR relate to CRs?

Below a few GeV, the local spectrum of CRs is affected by the solar wind and the Earth’s magnetic field, its modelling is elaborate. Above ~ 5 GeV, the spectrum of CR electrons, shown in Fig. 4, is well fit by a power law [26]: $dF/dE \propto E^{-\beta_e}$, with $\beta_e \approx 3.2 \pm 0.1$. The nuclear CR spectrum, above ~ 10 GeV and up to the “knee” at $\sim 3 \times 10^6$ GeV, is also a single power law: $dF/dE \propto E^{-\beta_p}$, with $\beta_p \approx 2.70 \pm 0.05$.

As discussed in detail in Section 7.1, CBs accelerate the ISM electrons and nuclei they encounter in their path as a “magnetic-racket” would, imparting to all species the same distribution of LFs γ . This means that the **source** spectra of (relativistic) nuclei and electrons have the same energy dependence: $dF/dE \propto E^{-\beta_s}$, with a species-independent β_s . The observed spectra are not the source spectra. The nuclear flux is modulated by the energy dependence of the CR confinement-time, τ_{conf} , in the magnetized disk and halo of the galaxy, affecting the different species in the same way, *at fixed E/Z*, with Z the nuclear charge. Confinement effects are not understood, but observations of astrophysical plasmas and of CR abundances as functions of energy suggest [27]:

$$\tau_{\text{conf}} \propto (Z/E)^c, \quad (2)$$

with $c \sim 0.5 \pm 0.1$ at the low energies at which the CR composition is well measured. This means that $\beta_s = \beta_p - c \sim 2.2$, as in footnote 1.

Above a few GeV, the electron spectrum is dominantly modulated by ICS on starlight and on the microwave background radiation, the corresponding electron “cooling” time being shorter than their confinement time. For an equilibrium situation between electron CR generation and ICS cooling, this implies that $\beta_e = \beta_s + 1 \sim 3.2$, a prediction [9] in perfect agreement with observation, as in Fig. 4. In the CB model, the Compton upscattered photons **are** the GBR, and their spectrum is a power law with a predicted [9] index $\beta_{\text{GBR}} = (\beta_e + 1)/2 \sim 2.1$, also in agreement with the data, as in Fig. 4. Cannonballs deposit CRs along their linear trajectories, which extend well beyond the Galaxy’s disk onto the halo and beyond.

The observed non-uniform (i.e. non-cosmological) distribution of GRB flux in intensity, latitude and longitude is well reproduced [9] for an ellipsoidal CR halo of –within very large errors– characteristic height ~ 20 kpc, and radius ~ 35 kpc.

6. The CR Luminosity of the Galaxy

If the CRs are chiefly Galactic in origin, their accelerators must compensate for the escape of CRs from the Galaxy to sustain the observed CR intensity: it is known from meteorite records that the CR flux has been fairly steady for the past few giga-years [28]. The conventional estimate of the CR luminosity of the Milky Way is [29]:

$$L_{CR} \sim 1.5 \times 10^{41} \text{ erg s}^{-1}. \quad (3)$$

In the CB model L_{CR} can be estimated from the electron CR density involved in its successful description of the GBR, if the local observed ratio of proton to electron fluxes is representative of the Galactic average. It can also be estimated from the rate of Galactic SNe and the typical energy in their jets of CBs. The results of these estimates agree [30], but they are over one order of magnitude larger than Eq. (3). This is not a contradiction, for the CB-model effective volume of confined CRs is much bigger than in the standard picture, wherein CRs are confined to the Galactic disk. The CB-model value of the CR confinement time is also one order of magnitude larger than the standard result, based on the ratios of stable to unstable isotopes [30]. This alterity is understood [31]: the stable CRs spend much of their time in the Galaxy’s halo, which in the CB-model is magnetized by the flux of CRs that the CBs deposit in it.

7. The Cosmic Ray Spectra

It is customary to “renormalize” the energy calibration of different experiments to make flux measurements look in better agreement; and to present the data as the flux times a power of energy, to emphasize the “features” of the spectrum and its changes of power “index”. This is done in Fig. 5 for the “all-particle” spectrum [32], showing the “knee” at $(2 \text{ to } 3) \times 10^{15}$ eV, the “second knee” at $\sim 5 \times 10^{17}$ eV and the “ankle” at

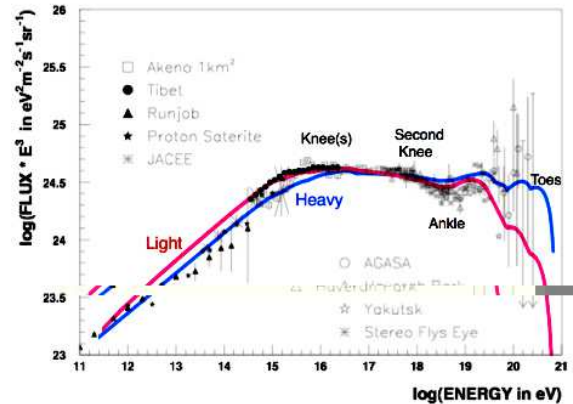


Figure 5. The “all-particle” CR spectrum. The “light” and “heavy” lines are predictions for the two CR abundances discussed in Section 7.9. Only one parameter was adjusted, see Section 7.5.

$\sim 3 \times 10^{18}$ eV. The purpose of this section is to outline how these features, and the changes of CR composition with energy, are simple consequences of the CB model of CR production.

7.1. “Collisionless magnetic rackets”

In an elastic collision of a relativistic CB of LF γ with (much lighter) ISM electrons or ions at rest, the light recoiling particles (of mass M) have an energy spectrum extending up to $E = 2\gamma^2 M c^2$. This is a *magnetic-racket accelerator* of gorgeous efficiency: the ISM particles reach up to $\Gamma = 2\gamma^2$. Single elastic scattering of target particles at rest is not the whole story, for CBs may collide with previously-accelerated CRs. Also, as in footnote 1, CBs may internally “Fermi”-accelerate particles, before reemitting them. The extreme in which the first process is dominant has been studied by Dar [12]. Here, the opposite extreme [13] is discussed. A bit coincidentally, the two extremes lead to very similar results.

In our study of GRB AGs, we assumed that the AG is dominated by electron synchrotron radiation in the magnetic field of Eq. (1). We also used the simplifying assumption that half of the electrons within a CB are unaccelerated, while the other half are accelerated, in the CB’s

rest system, to a source spectrum $dN/d\gamma_e \propto \gamma_e^{-\beta_s} \Theta(\gamma_e - \gamma)$, with $\beta_s = 2.2$ (as in footnote 1), and $\gamma = \gamma(t)$ the LF or the incoming electrons: the one of the CB in the SN rest system. This leads to the prediction of a wide-band AG spectrum in excellent agreement with observations [8]. Here, I make similar assumptions: the LF distributions of the ISM nuclei intercepted, magnetically deflected, partially accelerated and reemitted by a CB are *identical* to those of electrons (but for the effect of electron cooling by synchrotron radiation). The only other difference is that we shall discuss nuclei of up to very high energies, for which the “Larmor” limit —on the maximum possible acceleration within a CB— plays a role.

7.2. Elastic scattering: the “knees”

Let m be the proton mass and $\sim mA$ that of a nucleus of atomic weight A . The ISM nuclei recoiling from an elastic scattering with a CB of LF γ have energies in the range $mA \leq E_A \leq 2mA\gamma^2$. The initial LFs of CBs, extracted from the analysis of their AGs [7,8] and/or “peak energies” [4,5] peak at $\gamma_0 \sim 10^3$ and have a narrow distribution extending up to $\gamma_0 \sim 1.5 \times 10^3$. Thus, the spectrum of nuclei elastically scattered by CBs should end at an energy:

$$E[\text{knee}] \sim (2 \text{ to } 4) 10^6 A \text{ GeV}. \quad (4)$$

We shall see anon that $E[\text{knee}]$ is also the position at which the spectrum of inelastically scattered nuclei changes its slope.

The individual spectra of abundant CR elements and groups are shown in Fig. 6. Preliminary CR composition data from KASCADE [33] indicate that there is a change of slope of the individual spectra at the values predicted in Eq. (4), but the data are not yet good enough to establish the predicted linear A -dependence, or to distinguish it from a putative Z -dependence.

7.3. “Accelerated scattering”: the “toes”

The spectrum of Fermi-accelerated particles within a CB cannot extend beyond the Z -dependent energy at which their Larmor radius in the CB-field of Eq. (1) is larger than the CB’s radius. For typical parameters:

$$E[\text{Larmor}] \simeq 9 \times 10^{16} Z \text{ eV} \frac{B_{CB}[\gamma_0]}{3 \text{ G}} \frac{R_{CB}}{10^{14} \text{ cm}}. \quad (5)$$

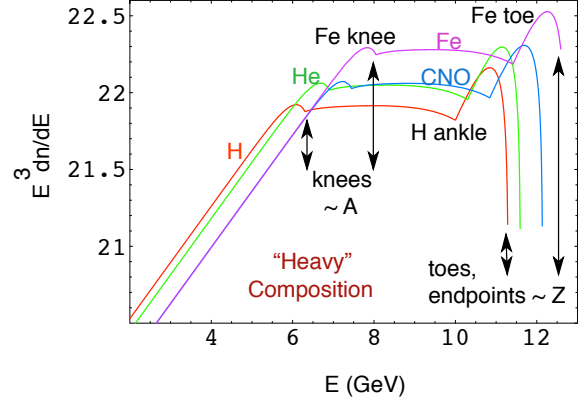


Figure 6. Log-log plot of the predicted $E^3 dN/dE$ spectra of H, He, the CNO group and the Fe group, for the “heavy” CR relative abundances of Section 7.9. The relative abundances become more “metallic” at the knees and again above the ankle. Only one parameter was adjusted.

The ISM nuclei exiting a CB after having being accelerated within it have energies extending up to $E[\text{toe}] = 2\gamma_0 E[\text{Larmor}]$, that is:

$$E[\text{toe}] \sim (2 \text{ to } 6) 10^{11} Z \text{ GeV}, \quad (6)$$

which is the maximum energy to which the CB mechanism we have discussed is capable of accelerating CRs. Notice that the predicted “toes” at the spectral end scale as Z , not like A , as the “knees” do, as illustrated in Fig. 6.

The energy $E[\text{toe}]$ for Fe nuclei is comparable to the maximum observed ones in CRs. There is some evidence [34] for changes of composition above the ankle, compatible with those implied by Fig. 6. But the extraction of relative CR abundances at very high energies is a difficult task.

7.4. The deceleration of CBs in the ISM

Consider a CB of initial mass M_0 , traveling through the ISM at an instantaneous LF γ . Let a be the ratio between the average energy of a nucleus exiting a CB in its rest system and the energy at which the nucleus entered, so that $\langle \gamma_{out} \rangle \equiv a\gamma$. For elastic scattering, $a = 1$; for nuclei fagocitated by the CB, $a = 0$; and for those Fermi-accelerated within the CB, $a > 1$. Let \bar{a}

be the mean value in the average over these processes, and \bar{A} the mean weight in the ISM density distribution dn_A . For $\gamma^2 \gg 1$, energy-momentum conservation implies a CB's deceleration law:

$$\frac{d\gamma}{\gamma^k} \simeq -\frac{m}{M_0} \gamma_0^{\bar{a}-1} \bar{A} dn_A, \quad k \equiv 3 - \bar{a}. \quad (7)$$

To compute the spectrum of the CRs produced by a CB in its voyage through the ISM we have to let the CB decelerate from $\gamma = \gamma_0$ to $\gamma \sim 1$, tantamount to integrating the CR spectra at local values of γ with a weight factor $dn_A \propto d\gamma/\gamma^k$.

The value of k in Eq. (7) cannot be ascertained with confidence. One reason is the averaging over the quoted processes. Three other reasons are: 1) The nucleus-CB elastic scatterings may not be isotropic. If the cross-section is modeled as a power-law in momentum transfer, $d\sigma \propto (1 + \beta \cos \alpha)^{-a_1}$, one obtains an approximate “effective” deceleration law $d\gamma/\gamma^{k_1}$, with $k_1 > k$. 2) The reemission of accelerated nuclei may be delayed, so that they exit the CB at $\gamma_{exit} < \gamma$. If the γ_{exit} distribution is modeled as a power law, $\gamma_{exit}^{-a_2}$, one obtains again an approximate “effective” deceleration law $d\gamma/\gamma^{k_2}$, with $k_2 > k$. 3) Slow CBs would be unobservable in GRBs or their AGs, for the fluences are biased towards large γ . Microquasars may also contribute low- γ_0 CR-generating CBs. If the γ_0 distribution is modeled as a power law, once again the “effective” value of k is increased. All in all, we may expect $k \sim 3$, but we cannot predetermine its value.

7.5. Spectrum of elastically-scattered CRs

Let the elastically scattered CRs, exiting a CB in its rest system with the decelerating instantaneous value of γ , be isotropically emitted, with a constant $d\sigma/d\cos\alpha$: we have seen that a reasonable non-isotropy only leads to an increase of k . Boosted by the CB's motion, the instantaneous CR spectrum in the SN rest system is:

$$\begin{aligned} \frac{dN}{d\gamma_A} &\propto \int_{-1}^1 \frac{d\cos\alpha}{2} \delta[\gamma_A - \gamma\gamma(1 + \cos\alpha)] \\ &= \frac{1}{2\gamma^2} \Theta[2\gamma^2 - \gamma_A]. \end{aligned} \quad (8)$$

To obtain the total “elastic” CR spectrum, in-

tegrate over the CB's trajectory:

$$\int_{\text{traj}} dn_A \frac{dN}{d\gamma_A} \propto \int_1^{\gamma_0} \frac{d\gamma}{\gamma^k} \frac{dN}{d\gamma_A} \propto \quad (9)$$

$$\left[\frac{1}{\gamma_A} \right]^{\frac{k+1}{2}} \left[1 - \left(\frac{\gamma_A}{2\gamma_0^2} \right)^{\frac{k+1}{2}} \right] \Theta[2\gamma_0^2 - \gamma_A]. \quad (10)$$

This elastic-scattering contribution extends up to $\gamma_A = 2\gamma_0^2$, as announced in Section 7.2. For energies below these knees, the Galaxy confines CRs so that the result of Eq. (10) is to be modified by the multiplicative factor $\propto 1/\gamma_A^c$ of Eq. (2). The observed slope $\beta \sim 2.7$ of the CR spectra below the knees is reproduced for $c + (k + 1)/2 = \beta$. In practice, this combination of parameters is the *only quantity* chosen by hand in predicting the all-particle and individual CR spectra.

7.6. The spectrum of CB-accelerated CRs

The spectrum of nuclei accelerated within a CB is “flavour-blind” in the variable γ_A , and of the form $dN/d\gamma_A \propto \gamma_A^{-\beta_s} \Theta(\gamma_A - \gamma) \Theta(b\gamma - \gamma_A)$, with $\beta_s = 2.2$, and $\gamma = \gamma(t)$. The second Θ function is the Larmor cutoff, for typical parameters $b \sim 10^5$. Boosted to the SN rest system, the instantaneous CR spectrum is:

$$\begin{aligned} &\int_{\gamma}^{b\gamma} \frac{d\bar{\gamma}}{\bar{\gamma}^{\beta_s}} \int_{-1}^1 \frac{d\cos\alpha}{2} \delta[\gamma_A - \bar{\gamma}\gamma(1 + \cos\alpha)] \\ &= \int_{\text{Max}[\gamma, \sqrt{\gamma_A/(2\gamma)}]}^{b\gamma} \frac{d\bar{\gamma}}{\bar{\gamma}^{\beta_s}} \frac{1}{2\bar{\gamma}\gamma}. \end{aligned} \quad (11)$$

This spectrum must still be integrated over the CB's trajectory, as in Eq. (9), and corrected for confinement in the Galaxy. The result is again simple and analytical, but a bit long to report here. Below the knee, it has the same power-law behaviour as the elastic contribution. The effect of the discontinuity in the lower limit of integration in Eq. (11) survives in the trajectory-integrated result as a predicted smooth change in slope by $\Delta\beta \sim 0.3$ at $\gamma_A = 2\gamma_0^2$, which is what is observed, see Figs. 5,6. The spectra extend all the way to the Larmor cutoff(s) of Eq. (5).

7.7. Galactic confinement: the ankle(s)

The interpretation of the ankle(s) in the CB model is conventional: they are the Z -dependent

energies at which the Galaxy and its magnetized halo no longer confine cosmic rays [2]. For $B \sim 3 \mu\text{G}$, the position of the ankle(s) is at:

$$E[\text{ankle}] \sim 3 \times 10^9 Z \text{ GeV}. \quad (12)$$

Cannonballs deposit CRs along their trajectories, reaching the halo and beyond. Galactic CRs above $E = E[\text{ankle}]$ escape. Instead of a cutoff, a change to a harder spectrum is seen, which must therefore be an *extragalactic flux*. I have assumed in Figs. 5,6 that the spectrum of CRs above the ankles is the source spectrum, corresponding to a sharp transition from $c \sim 0.5$ to $c = 0$ in Eq. (2).

7.8. GZK modulations

Cosmic rays having travelled in intergalactic space along straight or curved trajectories for sufficiently long times should be subject to rather sharp energy-cutoffs: the GZK effect [35]. Such cutoffs would act as “chinese-lady’s shoes” further constraining the “toe-nail” cutoffs we discussed. Are these GZK cutoffs expected in the CB model? It depends on Galactic “accessibility”.

It is difficult to ascertain the probability that extragalactic CRs of energies *below* the ankle penetrate the Galaxy, if only because in the CB-model there is an exuding Galactic “wind” of CRs and their accompanying magnetic fields. If the Galaxy is quite “accessible”, a good fraction of the observed lower-energy CRs would be extragalactic (not a dominant fraction, for otherwise redshift effects would erase the sharp features of the spectrum). A large extragalactic contribution implies long “look-back” times and, consequently, potentially observable GZK modulations. A small contribution implies short look-back times, no GZK effects, but the possibility of observing relatively well-located point sources in the Virgo-cluster “neighbourhood”. Thus, in a sense, this is a “no-lose” situation: some new effect ought to be found at the highest energies.

7.9. CR abundances

Let n_A be the number density of the “target” ISM nuclei converted by the CBs’ passage into CRs. The source spectra $dn_A/d\gamma$, are flavour-blind, so that the CR confinement-modified en-

ergy spectra are of the form:

$$\begin{aligned} \frac{dN_A}{dE} &\propto \frac{1}{Am} \frac{dn_A}{d\gamma} \left(\frac{Z}{E}\right)^c \\ &\propto K n_A A^{\beta-c-1} Z^c E^{-\beta}, \end{aligned} \quad (13)$$

with K a universal, composition-independent constant. Below the knee(s) $\beta = 2.7$ and $c \sim 0.5$ (I have ignored a weak composition-dependence of β , discussed by Dar[12]). In Fig. 7 the observed abundances of the most relevant *primary* CRs, up to Ni, are compared with the *solar* abundances, which are used as input to Eq. (13), whose results are also shown. In Figs. 5 and 6, I have referred to the predicted and observed compositions of Fig. 7 as “light” and “heavy”. The predictions are seen to fail at the large-metallicity end by a factor of ~ 3 . This is what is expected, for CBs travel much of the time in a star-burst region and a local superbubble that are known (within very large errors) to have thrice the metallicity of the solar neighbourhood. Given this uncertainty, it may be premature to do a complete calculation taking into account CR propagation and the production of CRs with a broad spectral distribution at the different points of many CB trajectories crossing a variety of ISM domains. After all, our aim is to understand all of the salient features of the CR conundrum, not its nitty-gritty details!

8. Conclusions and further predictions

A large variety of high-energy astrophysical phenomena are interrelated, and easy to understand in extremely simple terms [13]. The unifying concept is the ejection of relativistic blobs of matter in violent processes of accretion onto compact objects. The inspiring observations are those of quasars and microquasars. We have assumed that SNe axially eject very relativistic CBs of ordinary plasma, as their finite supply of matter catastrophically accreting onto their central compact object is used up. This assumption, complemented by a variety of observations of pre-SN environments, explains not only the SN/GRB association, but the properties of GRBs and XRFs [5]. The underlying process is ubiquitous in astrophysics: (inverse) Compton scattering. None of the parameters involved in these predictions

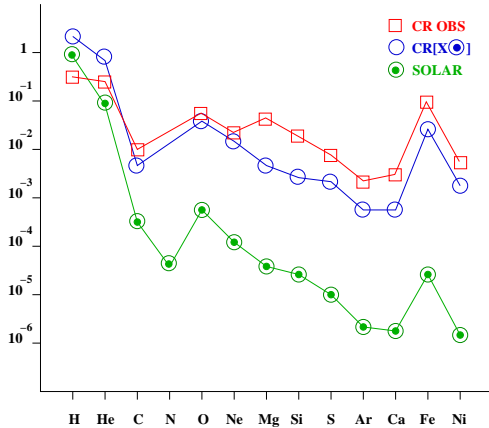


Figure 7. The relative abundances of primary CRs, from H to Ni. The (green) dotted circles are solar-neighbourhood ISM abundances. The (blue) circles are the predictions, with input solar abundances. The (red) squares are observed CR abundances below ~ 1 TeV.

are put in by hand: they rely on observations (e.g. the early luminosity of a SN), or are borrowed from the CB-model analysis of GRB AGs (the distribution of CB Lorentz factors and of the CB-motion angles relative to the line of sight to local observers, and the typical mass of a CB).

The analysis of GRB AGs requires extra assumptions that are no doubt over-simplifying: the way a relativistically expanding blob of plasma reaches an equilibrium radius as the process of radial reemission of the “collisionlessly” scattered charged ISM particles quenches the expansion, and the way in which the CB’s magnetic-field pressure thereafter compensates the inwards force of the radially exuding particles. But the ensuing description of AGs as the synchrotron radiation from the ISM electrons entering the CBs is simple and successful: the AG light curves and wide-band spectra of all GRBs of known redshift are well fit and, when predicted, correct.

Several predictions of the CB model of GRBs, we contend, are supported by the data, but require further corroboration. One is the hyperluminal motion of the CBs themselves [4,36], which may be easier to detect in XRFs: when not too

far, they are simply GRBs seen at larger angles. Another prediction concerns the AG X-ray lines, which in the CB model are not the generally-assumed lines of Fe and other intermediate elements, but the highly Doppler-boosted lines of light elements, notably H Ly- α lines [37]. Since CBs decelerate in the ISM as they emit these radiations, the lines should evolve towards lower frequencies in a predicted fashion [37].

On the basis of much less observational input, we propose [5] that short-duration GRBs are associated with Type Ia SNe (30% of the SNe are of this type, 30% of GRBs are short). If the observers did not give up so early in attempting to discover the weak AG of short GRBs—but waited for a few weeks for the peak SN light—the SN ought to be observable. That would be good news for cosmology, even if GRB-associated Type Ia SNe deviate from the usual “standard candle” properties: in the CB model SNe are roughly axially—but not spherically—symmetric. SN1998bw and the other almost identical SNe associated with GRBs (some spectroscopically established), are ordinary SNe seen very close to their axis. Both Type Ia and core-collapse SNe (at least of Type Ib,c) ought to be closer to standard “torch-lights” than to “candles”.

We have also seen that the CB-model explains the shape of the CR electron spectrum, and the related spectrum and angular distribution of the GBR, most of which is not “cosmological”: it is associated at high latitudes with our own Galactic halo. Higher-energy data on CR electrons and the GBR might confirm the model by discovering the predicted “knees” in the corresponding spectra [9]. Seeing the “GBR” light from the halo of Andromeda would also be quite a coup [9].

In the CB model, there are no Cooling Flows, but “Warming Rays” in dense X-ray emitting clusters. It is the mysterious mechanism of *heating* that we identified: CB-induced CRs [11].

The CB model of CRs is rather successful, considering that only one parameter was adjusted. Clearly the results could be improved, as better data are gathered (e.g. on composition at all energies above ~ 1 TeV). Many simplifying choices were made: a spatially constant ISM composition, a 50-50 contribution of nuclei accelerated

and unaccelerated within a CB, a naïve energy dependence of the Galactic-confinement factor... Even so, the distribution of CRs in the Galaxy, their total luminosity, the broken power-law spectra with their observed slopes, the position of the knee(s) and ankle(s), and the alleged variations of composition with energy are all explained in terms of simple physics. Surely, “life” may be more complicated, e.g. nearby SNe could contribute low-energy CRs, accelerated by conventional shock mechanisms. There is no CB-model-specific prediction concerning CRs, except that they are deposited along very long lines exiting star-death regions, as opposed to points in these regions, as in standard models. This prediction might be testable in the search for line inhomogeneities in the radiation from CR electrons.

The CB model is not a *theory* of practically all high-energy astrophysical phenomena. It is lacking a deeper theoretical understanding of the magneto-dynamics within a CB; and of *cannons* themselves: the engines generating the mighty ejections of compact astrophysical objects.

REFERENCES

1. A. Dar et al., *ApJ* **388**, 164 (1992).
2. A. Dar and R. Plaga, *A&A* **349**, 259 (1999).
3. N. J. Shaviv and A. Dar, *ApJ* **447**, 863 (1995).
4. A. Dar and A. De Rújula, astro-ph/0008474.
5. A. Dar and A. De Rújula, astro-ph/0308248, to be published in *Phys. Repts.*
6. S. Dado, A. Dar and A. De Rújula, *A&A* **422**, 381 (2004).
7. S. Dado, A. Dar and A. De Rújula, *A&A* **388**, 1079 (2002).
8. S. Dado, A. Dar and A. De Rújula, *A&A* **401**, 243 (2003).
9. A. Dar and A. De Rújula, *MNRAS* **323**, 391 (2001).
10. A. Dar and A. De Rújula, *ApJ* **547**, L33 (2001).
11. S. Colafrancesco, A. Dar and A. De Rújula, *A&A* **413**, 441 (2004).
12. A. Dar, astro-ph/0408310.
13. A. De Rújula, astro-ph/0411763.
14. A. S. Wilson, A. J. Young and P. L. Shopbell, *Astrophys. J.* **547**, 740 (2001).
15. I. F. Mirabel and L. F. Rodriguez, *Ann. Rev. Astron. Astrophys.* **37**, 409 (1999).
16. T. Kotani et al., *Publ. Astron. Soc. Jap.* **48**, 619 (1996).
17. A. De Rújula, *Phys. Lett.* **B193**, 514 (1987).
18. P. Nisenson and C. Papaliolios, *Astrophys. J.* **518**, L29 (1999).
19. J. K. Frederiksen et al., *Astrophys. J.* **608**, L13 (2004).
20. P. Grandi et al., *Astrophys. J.* **586**, 123 (2003).
21. D. J. Thompson and C. E. Fichtel, *Astron. Astrophys.* **109**, 352 (1982).
22. P. Sreekumar et al., *Astrophys. J.* **494**, 523 (1998).
23. G. Bignami et al., *Astrophys. J.* **232**, 649 (1979).
24. D. N. Page and S. W. Hawking, *Astrophys. J.* **206**, 1 (1976).
25. A. Dar, A. De Rújula and N. Antoniou, astro-ph/9901004.
26. P. Ferrando et al., *Astron. Astrophys.* **316**, 528 (1996).
27. S. P. Swordy et al., *Astrophys. J.* **330**, 625 (1990).
28. M. S. Longair, *High Energy Astrophysics* (Cambridge Univ. Press, 1981).
29. L. O’C. Drury, W.J. Markiewicz, and H. J. Völk, *Astron. Astrophys.* **225**, 179 (1989).
30. A. Dar and A. De Rújula, *Astrophys. J.* **547**, L33 (2001).
31. R. Plaga, *Astron. Astrophys.* **330**, 833 (1998).
32. B. Wiebel-Sooth and P. L. Biermann, *Landolt-Börnstein*, (Springer, Heidelberg 1998).
33. A. Haungs et al., *Acta Phys. Polon.* **B35**, 331 (2004).
34. D. J. Bird et al., *Astrophys. J.* **424**, 491 (1994).
35. K. Greisen, *Phys. Rev. Lett.* **16**, 748 (1966); G. T. Zatsepin and V. A. Kuz’min, *JETP Lett.* **4**, 78 (1966).
36. S. Dado, A. Dar and A. De Rújula, astro-ph/0406325.
37. S. Dado, A. Dar and A. De Rújula, *Astrophys. J.* **585**, 890 (2003).